

# **Probing the interaction of SPIONs with various physicochemical properties and amyloid beta protein**

**By Morteza Mahmoudi**

**Grant Number 4765**

## **Materials and Methods**

Particles with various surface charges (i.e. negative, plain, and positive) and sizes were prepared according to the protocols reported elsewhere (Amiri, H., Wang, K., Mahmoudi, M., Monopoli, M., Lynch, I. Dawson, K. A., ACS Nano, submitted)

## **Amyloid Beta**

Amyloid peptide A $\beta$ (1-42) was synthesized by the W. M. Keck foundation, Biotechnology Resource Laboratory (Yale University), with an 80% purity (the remaining 20% of the lyophilized material is mainly water and some residual TFA).

A $\beta$ (1-42) was dissolved in a 50:50 mixture of 1%NH<sub>4</sub>OH and 100 mM Tris buffer followed by ultra-centrifugation (65 000 rpm; 1 000 000g) for 1 h at 4°C in a Beckman ultra-centrifuge in order to remove pre-existing amyloid fibrils, which are collected in the bottom of the vial; the upper 75% of the supernatant was carefully collected, and the concentration of A $\beta$ (1-42) was measured using the amount of absorbance at 275 nm according to the following equation:

$$C = A/\epsilon \quad (1)$$

Where C is the concentration in molar, A is the absorption (arbitrary units),  $\epsilon$  is an extinction coefficient (M<sup>-1</sup> cm<sup>-1</sup>). In order to make solutions with desired concentrations, the supernatant was diluted to 0.05-50  $\mu$ M using 13 mM sodium phosphate buffer, 0.02% NaN<sub>3</sub>, pH 7.4. This solution was used immediately for experiments.

## ThT Fluorescence Assay

A common method for evaluation (either *ex vivo* or *in vitro*) of the fibrillogenesis process is the Thioflavin T (ThT) fluorescence assay. ThT is a benzothiazole dye that exhibits enhanced fluorescence (with excitation and emission at 440 nm and 480 nm, respectively) upon binding to amyloid fibrils and protofibrils. The ThT fluorescence assays were conducted as described in several reports<sup>29, 44</sup>. For the continuous experiments, 90  $\mu$ l of the optimal concentration of A $\beta$ (1-42) with 200  $\mu$ M ThT per well was incubated in the absence or presence of various SPIONs (10  $\mu$ l of various iron concentrations (i.e. 40-100  $\mu$ g/ml), respectively) at several concentrations in 37°C and shaken at 700 rpm in a 96 well black fluorescence plate, NUNC 96 black polypropylene microwell plates, with shaking at 700 rpm in a plate reader (Varioscan Flash from Thermo Fischer). The ThT fluorescence was measured through the bottom of the plate every 20 min, from 20 min to 1340 min, (with the predetermined excitation and emission of ThT) with continuous shaking at 700 rpm and 37°C between readings. For the control wells, 10  $\mu$ l of solution without SPIONs (i.e. DI water) were added to the wells. Note that each experimental point is an average of the fluorescence signal from five wells containing aliquots of the same solution consisting of SPIONs and A $\beta$  or A $\beta$  in the absence of SPIONs.

To assess the effect of pH on A $\beta$  fibrillation (in the absence of SPIONs), A $\beta$  solutions of different pH (i.e. pH 2-12) were prepared by adding the acidic solution (i.e. sodium phosphate buffer) to the basic solution.

The obtained kinetic data were analyzed assuming the typical sigmoidal behavior in order to extract the kinetic parameters of the bimodal fibrillation processes. An empirical sigmoidal equation was used:<sup>45, 46</sup>

$$y = y_0 + \frac{y_{max} - y_0}{1 + e^{-\frac{(t-t_1)k}{2}}} \quad (2)$$

where  $y$  is the fluorescence intensity at time  $t$ ,  $y_0$  and  $y_{max}$  are the initial and maximum fluorescence intensities, respectively,  $t_{1/2}$  is the time required to reach half the maximum intensity, and  $k$  is the apparent first-order aggregation constant. In addition, the lag time can be defined using the following equation:

$$\text{lagtime} = t_{1/2} - \frac{2}{k} \quad (3)$$

It is worthwhile to note that we performed ThT fluorescence assays for SPIONs in the absence of A $\beta$ ; the results confirmed that there is no binding between ThT dye and SPIONs.

### **Circular Dichroism**

In order to probe the secondary structure of A $\beta$  after interaction with the various SPIONs, circular dichroism (CD) was employed, using an Aviv Model 202 CD spectrometer. CD spectra were recorded at room temperature; the wavelength step was 1nm, 3 scans were taken per sample in the range from 190 to 300 nm, and the averaging time was 1 s at each wavelength.

Potential scattering effects from the SPIONs were considered by running the CD spectra of the SPIONs in the absence of A $\beta$ .

### **Results**

TEM time-course images of the control sample (A $\beta$  in the absence of any SPIONs, at 0.5  $\mu\text{g}/\text{ml}$ ) are shown in Figure 1a-d for 700 min, 1200 min, 1800 min, and 2400 min incubation time. As seen, the fibrils have a very broad size distribution and low sizes in the early

fibrillation stage (Figure 1a); however, the size of the fibrils increases and their size distributions is significantly narrowed with increasing the incubation time. The blue arrows in Figure 1a show the small fibrils which would be degraded and attached to the larger one by increasing the incubation time. It is interesting to note that although ThT shows that the fibrillation process was finished after 800 min of incubation time (see Figure 2), TEM images revealed that a phenomena similar to Ostwald ripening is in progress over much longer times, leading to the domination of larger fibrils at longer times (since the total number of intercolation sites is the same, ThT does not have the capability to follow this process).

Addition of the negative and plain dextran coated SPIONs (both single and double layer), resulted in the size of the fibrils being significantly reduced and the fibril size distributions being narrower (see Figures 3 and 4). In both cases, we have observed inhibition of the fibrillation lag time in the ThT assay together with lower fibrillation rates. So we can conclude that negatively charged nanoparticles (plain is also slightly negative; see Table 1), can retard fibrillation process using their capability to make homogen growth in oligomerization phase. In comparison, positively charged particles caused the formation of fibrils with a very broad size distribution (see Figure 5). That may be a reason for their accelerating effect on the fibril elongation process.

According to the results obtained in our paper together with TEM, we can conclude that there would be a thermodynamically-driven spontaneous process in fibril formation which occurs due to the existence of different oligomers with various stabilities (see Figure 6). More specifically, larger fibrils are more energetically favored than smaller ones. This stems from the fact that molecules on the tail of the oligomers are energetically less stable than the ones in the interior (i.e. back bone of the oligomers or smaller fibrils); hence, as the system tries to lower its overall energy, amyloid monomers will tend to detach from the small fibrils and diffuse into the solution. When all small monomers do this, the concentration of soluble

amyloid increases in the solution, causing supersaturation phenomena. So, the free monomers have a tendency to be condensed onto the surface of larger fibrils. Therefore, all smaller fibrils shrink, while larger fibrils grow, and overall the average fibril size will be increased. After an infinite amount of time, the entire population of fibrils will have become one, huge, fibril to minimize the total energy of the solution. We are introducing new equation which would be comprehensively enhanced in future:

$$t_{lag} \propto \frac{1}{\langle R \rangle^n C^\varphi} \quad (5)$$

Where  $\langle R \rangle$  is size distribution of the fibrils,  $C$  is the concentration of soluble  $A\beta$  monomers,  $n$  and  $\varphi$  are exponents which should be defined according to the type and physiochemical properties of the particle additives.

In order to probe the effect of SPIONs on any secondary structural changes of A $\beta$ , far-UV CD spectroscopy was employed. The results are shown in Table 3 (Examples of the circular dichroism signature are shown in Figure 7). The CD spectra of monomeric (random coil structure) A $\beta$  have a characteristic, intense minimum and a maximum near 200 and 220 nm, respectively; observations that are consistent with a random coil conformation. After the full fibrillation of the monomers (i.e. 1340 min) at 37°C, the CD spectrum revealed the changes in the wavelength and intensities, due to the changes in secondary conformation, confirming the formation of the  $\beta$ -sheet conformation ( $\beta$ -sheet-rich assemblies; minimum wavelength at 214 nm). CD spectra results of the positive particles, which confirm the ThT fluorescence results, show the formation of severe  $\beta$ -sheet assemblies regardless of the size of particles. In contrast, negative and fairly plain dextran coated SPIONs illustrate the characteristics of the random coil, suggesting no induction of conformational change by the bare SPIONs. It is interesting to note that the CD spectra showed the same trends with the ThT fluorescence results. The obtained results are fully consistent with the previous reports on the CD study of various employed molecules/particles for retardation and acceleration of lag time in A $\beta$  proteins<sup>62</sup>.

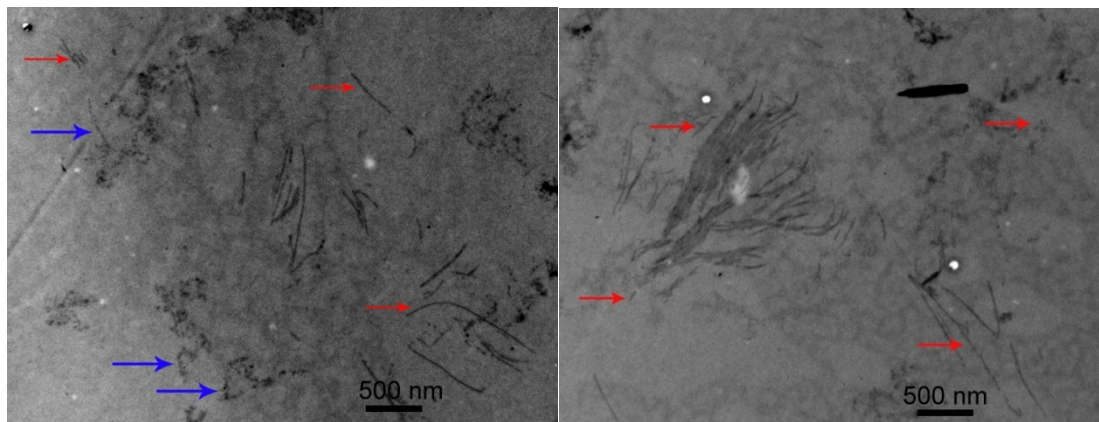
**Table 3:** Wavelength and corresponding minimum and maximum ellipticities of CD spectra of A $\beta$  alone, various SPIONs alone, and the mixtures of A $\beta$  and different concentrations of various SPIONs

	Concentration	$\lambda$ (nm)	min/max [ $\theta$ ]	$\lambda$ (nm)	min/max [ $\theta$ ]
A $\beta$ (After 100 min incubation)	0.5 $\mu$ M	207	-2.81	222	-0.12
A $\beta$ (After 1340 min incubation)	0.5 $\mu$ M	200	3.06	215	-13.03
Bare (alone)	100 $\mu$ g/ml	195	-0.23	208	-2.5
Bare (with A $\beta$ )	40 $\mu$ g/ml	203	-31.95	215	2.86
	60 $\mu$ g/ml	205	-34.87	219	0.23
	80 $\mu$ g/ml	202	-30.34	217	2.95
	100 $\mu$ g/ml	201	-32.54	215	3.01
S-Negative (alone)	100 $\mu$ g/ml	195	-0.13	208	-2.3
S-Negative (with A $\beta$ )	40 $\mu$ g/ml	206	-12.29	220	-0.12
	60 $\mu$ g/ml	206	-12.32	221	-2.07
	80 $\mu$ g/ml	205	-12.12	220	-2.21
	100 $\mu$ g/ml	207	-12.38	220	-2.48
S-Plain (alone)	100 $\mu$ g/ml	193	0.16	207	-2.11
S-Plain (with A $\beta$ )	40 $\mu$ g/ml	203	11.98	217	-5.87

	60µg/ml	206	-11.98	220	-0.07
	80µg/ml	205	-11.65	220	-0.17
	100µg/ml	207	-18.35	222	-0.11
S-Positive (alone)	100µg/ml	196	-2.92	207	-0.21
S-Positive (with Aβ)	40µg/ml	204	-18.25	218	2.21
	60µg/ml	204	-29.83	219	2.11
	80µg/ml	201	-22.78	216	3.08
	100µg/ml	200	-39.46	215	3.17
L-Negative (alone)	100µg/ml	194	-0.28	209	-2.12
L-Negative (with Aβ)	40µg/ml	207	-10.04	220	-2.01
	60µg/ml	207	-9.07	222	-2.53
	80µg/ml	203	-25.23	217	2.56
	100µg/ml	202	-29.87	216	2.03
L-Plain (alone)	100µg/ml	193	+0.21	206	-1.93
L-Plain (with Aβ)	40µg/ml	207	-8.07	221	-2.54
	60µg/ml	207	-6.04	222	-2.65
	80µg/ml	206	7.01	221	-2.81
	100µg/ml	207	-5.01	222	-2.85

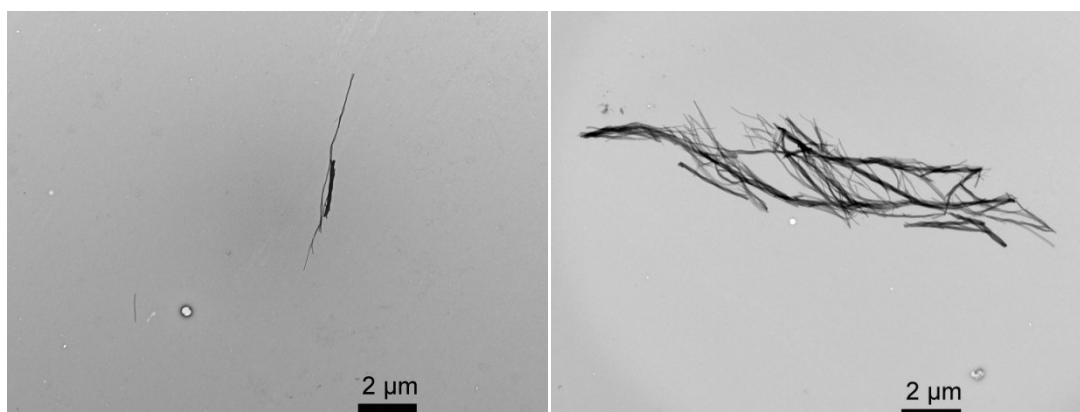


L-Positive (alone)	100 $\mu$ g/ml	195	-0.28	208	-1.9
L-Positive (with A $\beta$ )	40 $\mu$ g/ml	200	-32.98	215	3.17
	60 $\mu$ g/ml	201	-37.45	215	3.02
	80 $\mu$ g/ml	200	-43.23	215	3.12
	100 $\mu$ g/ml	200	-48.12	215	3.78



(a)

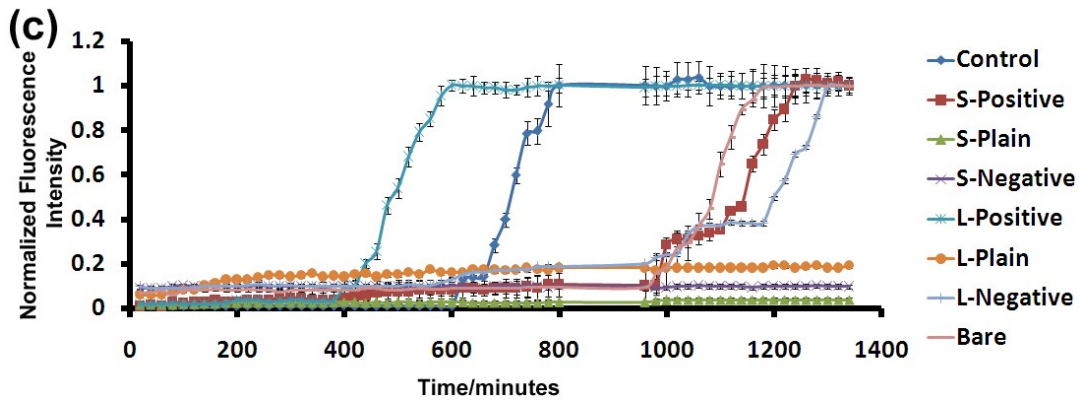
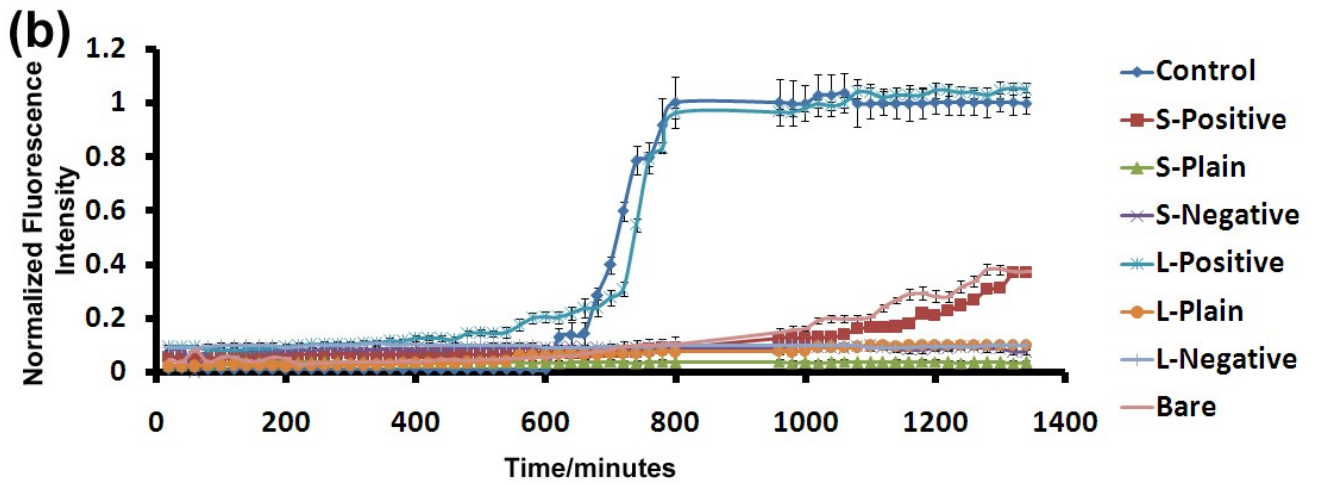
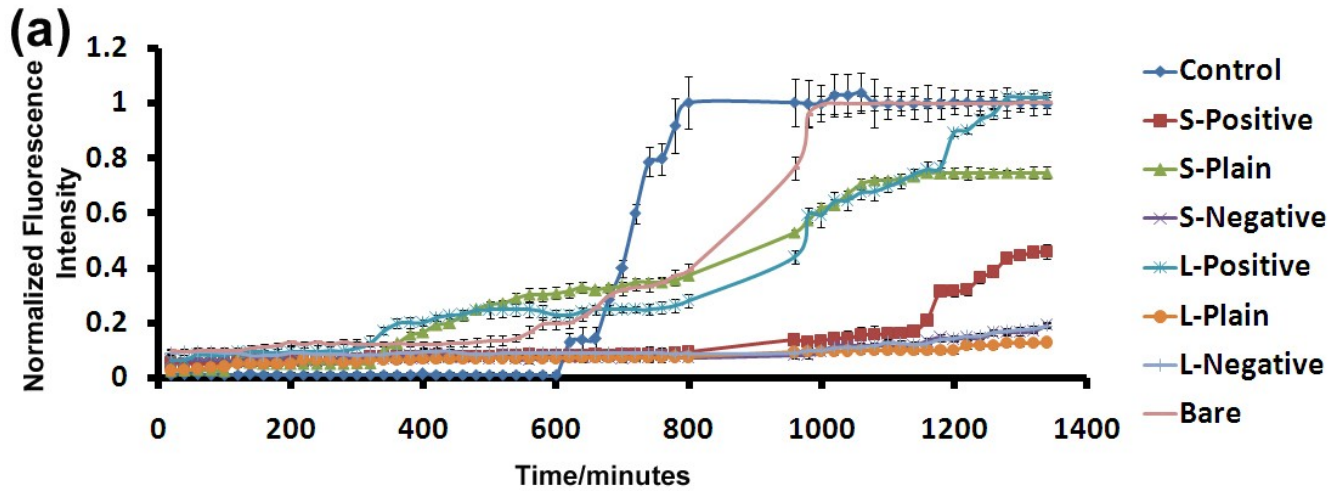
(b)



(c)

(d)

**Figure 1:** TEM images of A $\beta$  fibrils after incubation for (a) 700 min, (b) 1200 min, (c) 1800 min, and (d) 2400 min in the absence of any SPIONs. Protein concentration is 0.5  $\mu$ M.



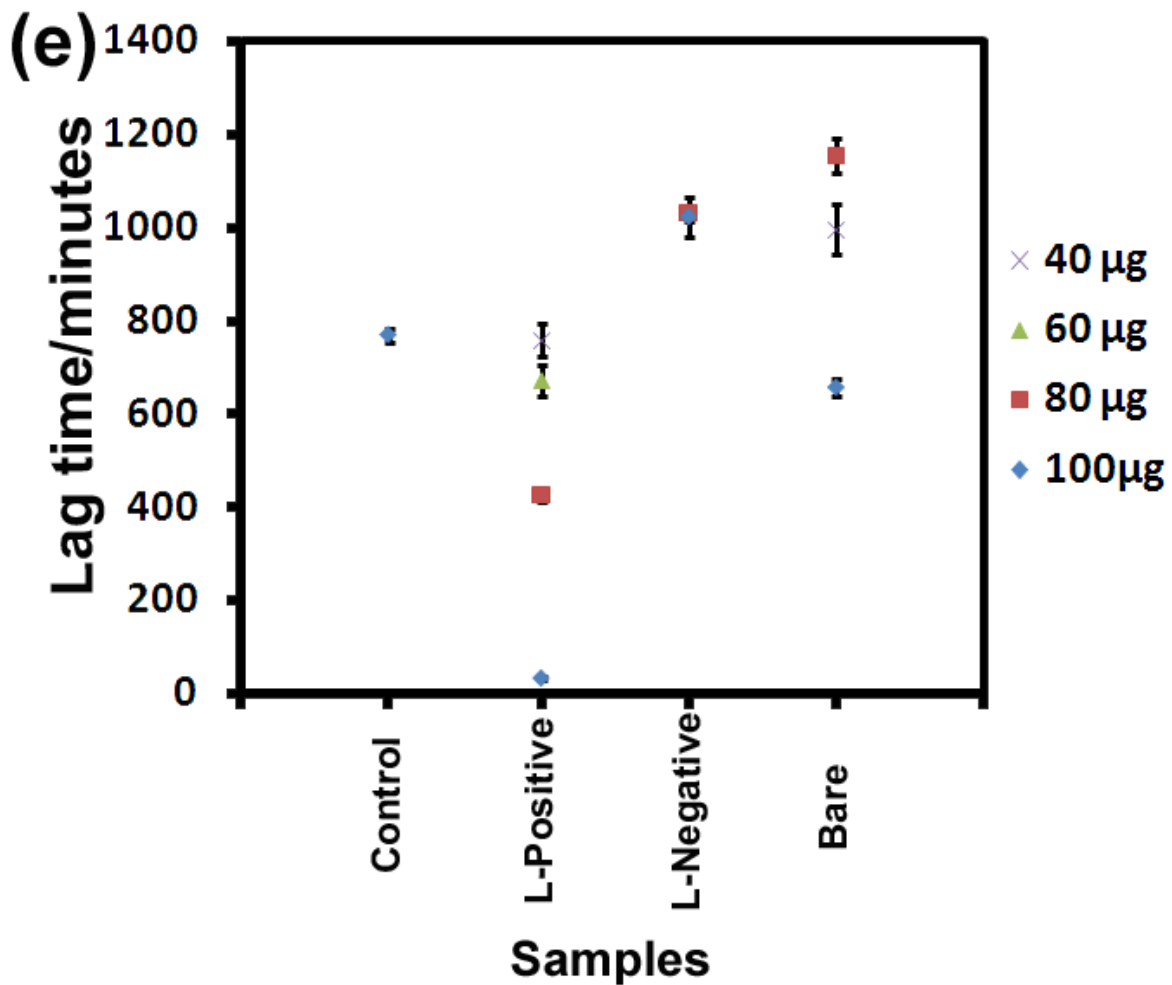
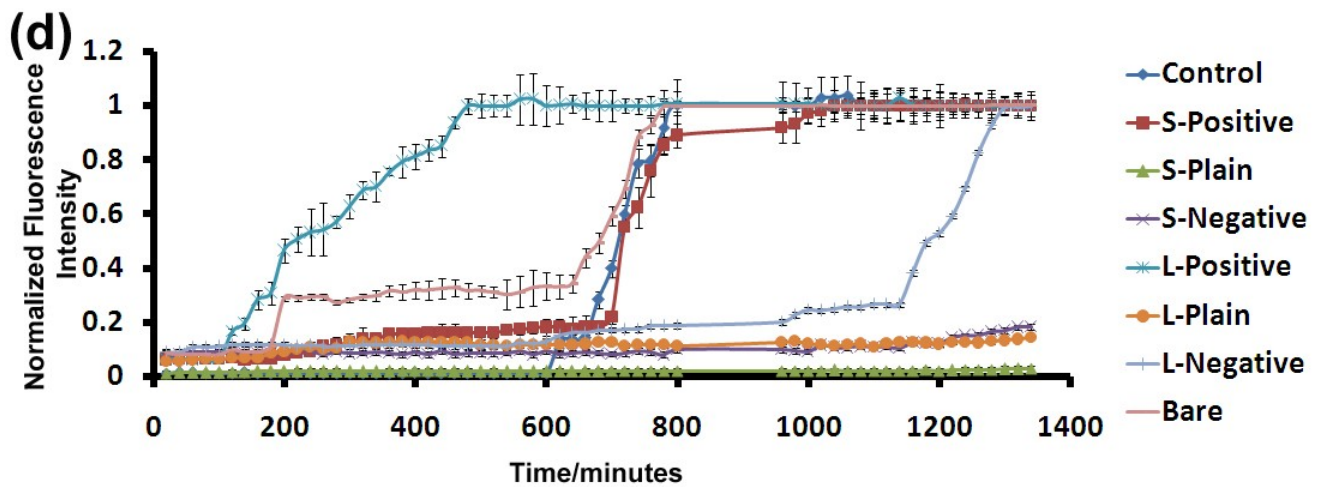


**Figure 2:** Kinetics of aggregation of Aβ in the absence or presence of various SPIONs at different concentrations including (a) 40μg/ml, (b) 60μg/ml, (c) 80μg/ml, and (d) 100μg/ml; (e) Lag times of Aβ fibrillation versus various SPIONs concentrations determined from the experiments shown in a-d.

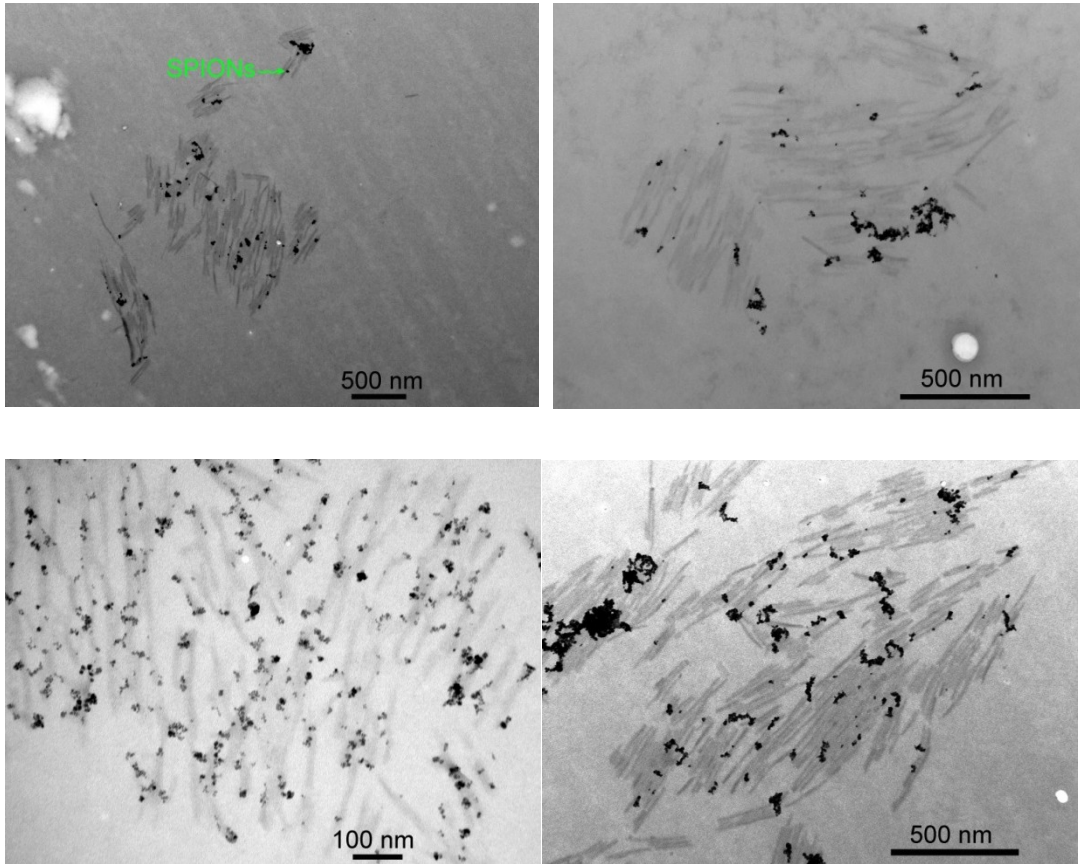


**Figure 3:** TEM images of A $\beta$  fibrils after incubation of A $\beta$  monomers (concentration of 0.5  $\mu$ M) with L-Negative SPIONs, with particles concentration of 100  $\mu$ g/ml, after incubation for 2400 min.

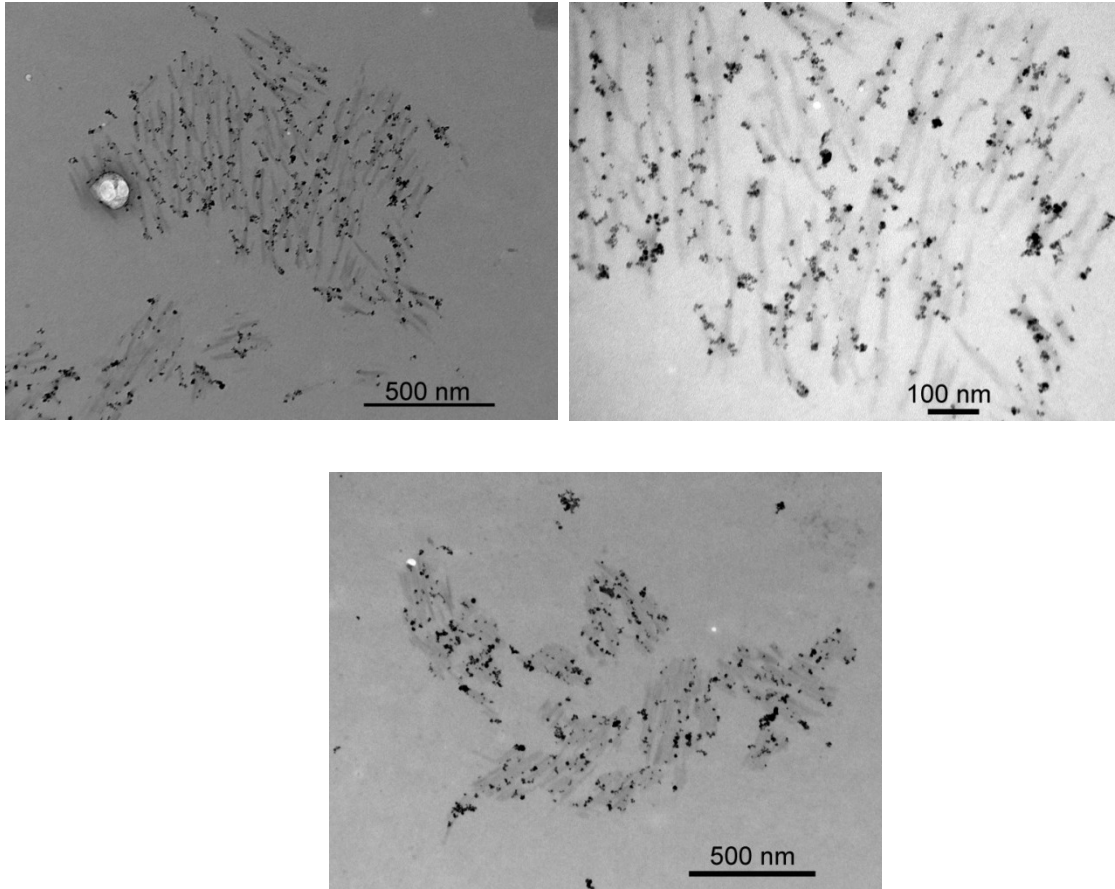


**Figure 4:** TEM images of A $\beta$  fibrils after incubation of A $\beta$  monomers (concentration of 0.5  $\mu$ M) with L-plain SPIONs, with particles concentration of 100  $\mu$ g/ml, after incubation for 2400 min.

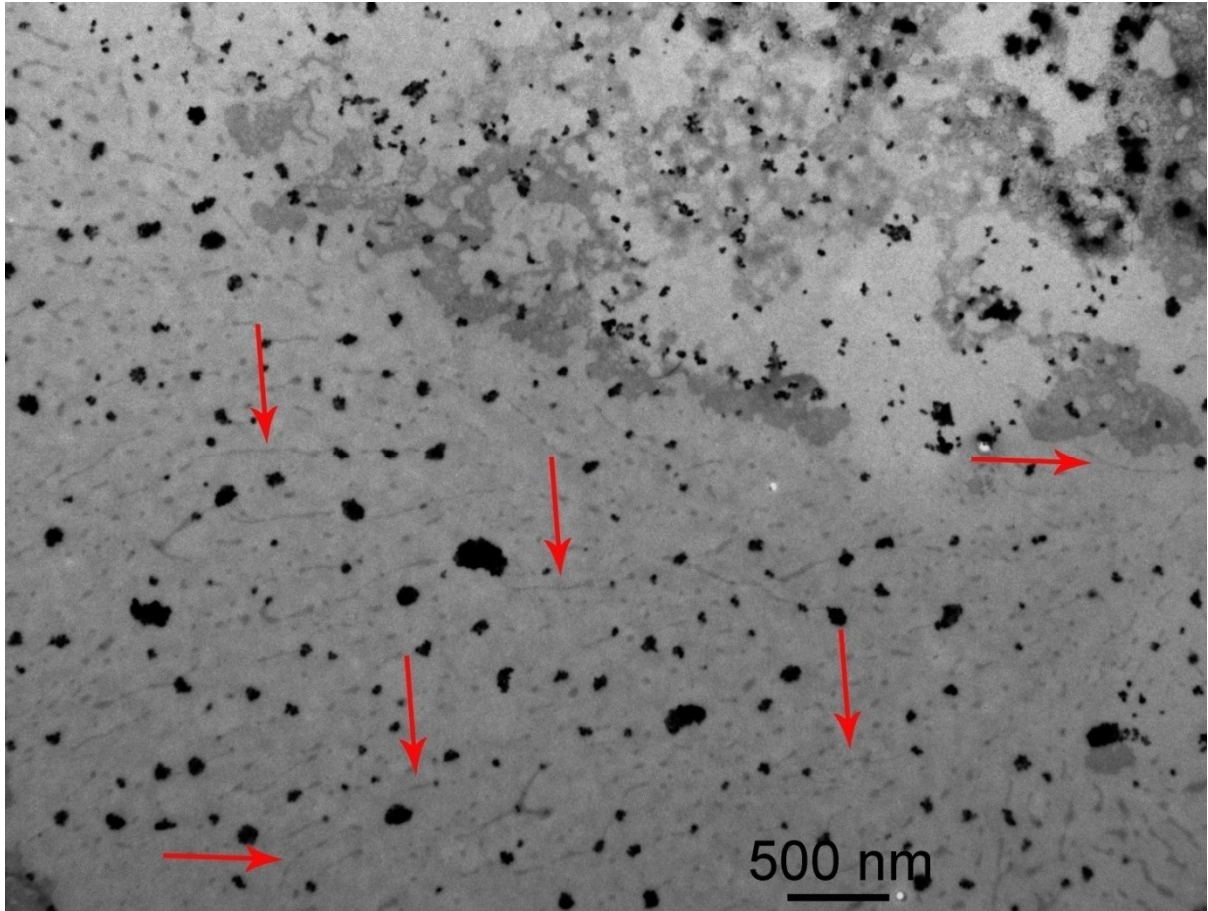


**Figure 5:** TEM image of A $\beta$  fibrils after incubation of A $\beta$  monomers (concentration of 0.5  $\mu$ M) with L-positive SPIONs, with particles concentration of 100  $\mu$ g/ml, after incubation for 2400 min. Only very small fibrils are observed (see red arrows)

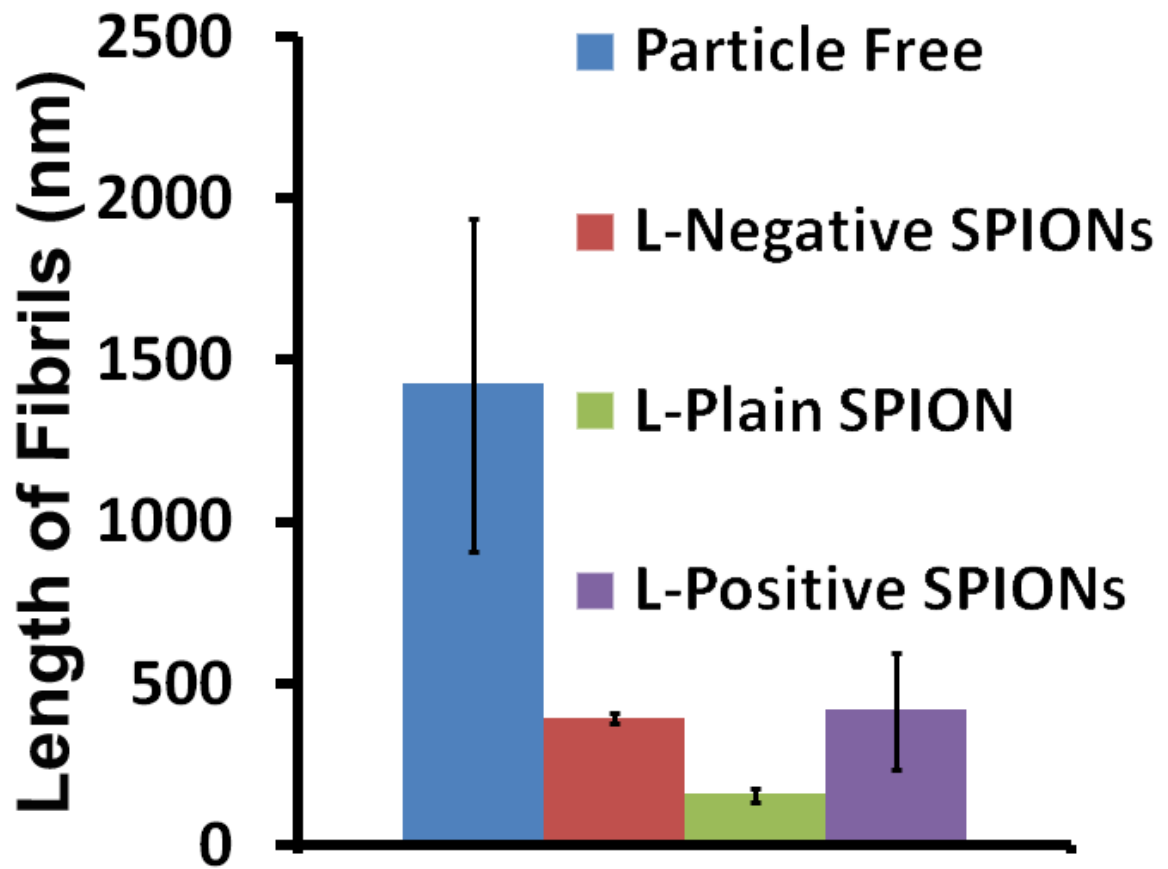


**Figure 6:** Size of A $\beta$  fibrils in various mediums (i.e. free from particles and medium containing L-Series of SPIONs); data obtained from TEM images.

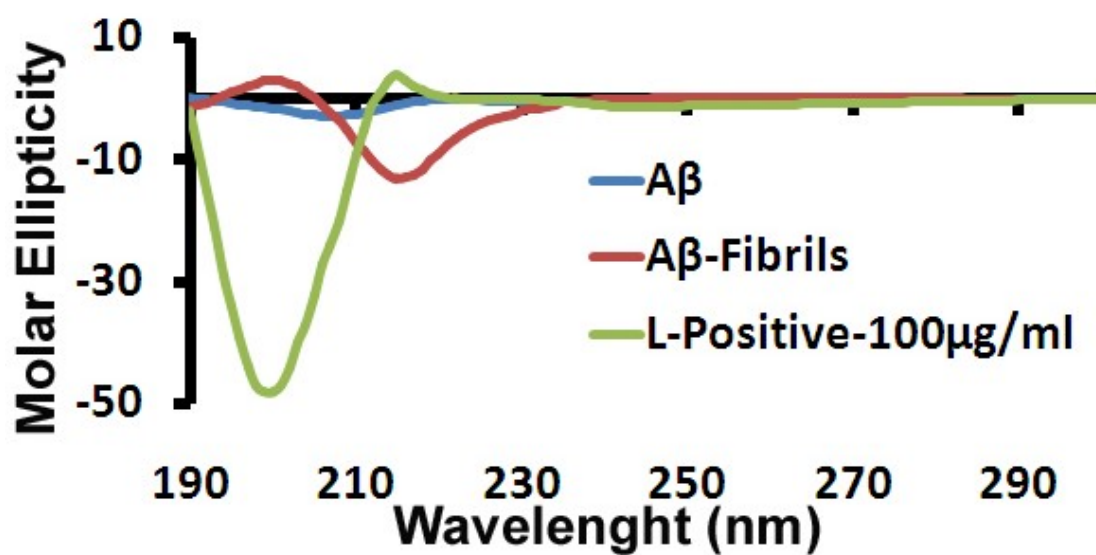


**Figure 7:** Circular dichroism signature obtained for A $\beta$ , which concentration of 0.5  $\mu$ M, alone after (a) 100min and (b) 1340 min incubation, and (c) a mixture of A $\beta$  and D-Positive SPIONs, with particles concentration of 100  $\mu$ g/ml, after 1340min.

The whole story has been submitted to *Langmuir*.



This document was created with Win2PDF available at <http://www.daneprairie.com>.  
The unregistered version of Win2PDF is for evaluation or non-commercial use only.